

Chemical principles for electroactive metal–organic frameworks

Aron Walsh, Keith T. Butler, and Christopher H. Hendon

Metal–organic frameworks (MOFs) are porous ordered arrays of inorganic clusters connected by organic linkers. The compositional diversity of the metal and ligand, combined with varied connectivity, has yielded more than 20,000 unique structures. Electronic structure theory can provide deep insights into the fundamental chemistry and physics of these hybrid compounds and identify avenues for the design of new multifunctional materials. In this article, a number of recent advances in materials modeling of MOFs are reviewed. We present the methodology for predicting the absolute band energies (ionization potentials) of porous solids as compared to those of standard semiconductors and electrical contacts. We discuss means of controlling the optical bandgaps by chemical modification of the organic and inorganic building blocks. Finally, we outline the principles for achieving electroactive MOFs and the key challenges to be addressed.

Introduction

Atomistic materials modeling has become a valuable tool in contemporary materials science. The accelerated characterization of known materials and the assessment of hypothetical systems are being supported by developments in software and hardware, including an international supercomputing infrastructure and a growing number of reliable simulation packages.¹ The predictive power of numerical simulation approaches, based on quantum mechanical description of solids, underpins the emerging field of computational materials design.²

While first-principles methodologies, for example, those based on density functional theory (DFT), were once limited to simple structures and compositions with tens of atoms in a crystallographic unit cell, modern computer architectures can support the direct simulation of thousands of atoms. The chemical and physical properties of metal–organic frameworks (MOFs) are now accessible to high-quality quantum mechanical simulations. In the past, simple empirical potentials proved useful for screening compositions and topologies in the context of gas storage.³ As interest in MOFs extends toward their physical properties and chemical reactivity, knowledge of the electronic structure becomes essential and crucial.

In this article, following a brief description of the common workflow for calculating the physical response functions of hybrid solids, we review recent progress in our understanding of the chemical bonding underpinning the electronic structure of MOFs. This includes the atomic and molecular orbitals that overlap

to form the valence and conduction bands, the electron addition and removal energies, and a set of design principles for tailoring the electronic and optical activity for functional devices.

From computer to properties Input: Crystal structure

A reliable structure is an essential starting point for quantum mechanical calculations of crystalline solids. The ground-state distribution of electrons is determined for a particular arrangement of ions in a lattice that extends infinitely across three spatial dimensions. The crystallography of MOFs is challenging: many reported structures contain solvent molecules, lattice sites with partial occupancy, or missing hydrogen atoms. In addition, high-symmetry space groups are usually assigned in the absence of hydrogen (due to their low electron density and weak diffraction intensity). The symmetry is often lowered when hydrogens are included, for example, when carbon atoms are replaced by the appropriate CH, CH₂, or CH₃ groups. One useful resource is the CoRE-MOF (computation-ready, experimental MOF) database⁴ that provides “simulation ready” structures and has been employed in high-throughput screening projects.⁵

A further concern, which has not been fully explored for MOFs, is that Bragg diffraction provides insights into the (spatial and temporal) average crystal structure, but the local environment may be quite different.⁶ For organic–inorganic solids, there is the possibility of vibrations, librations, and rotations of atoms or molecular units.^{7–10} Structural disorder

Aron Walsh, Department of Materials, Imperial College London, UK; a.walsh@imperial.ac.uk
Keith T. Butler, Department of Chemistry, University of Bath, UK; k.t.butler@bath.ac.uk
Christopher H. Hendon, Department of Chemistry, Massachusetts Institute of Technology, USA; hendon@mit.edu
doi:10.1557/mrs.2016.243

has been recognized as a potentially useful trait in framework materials,¹¹ but from the point of view of atomistic simulation of MOFs, it has been largely neglected up to this point.

Output: Physical properties

The crystal structures obtained from experiments are usually subject to local optimization for a chosen description of the interatomic interactions. The three lattice vectors and all lattice sites are minimized with respect to the external pressure and internal forces on the system. For a modern DFT exchange–correlation functional (e.g., PBEsol¹²), experimental and measured structural parameters usually agree to within several percent.

On the United Kingdom supercomputer ARCHER (advanced research computing high-end resource), which is representative of the current generation of national systems, a high-quality electronic structure calculation of a MOF with several hundred atoms in the unit cell will require up to 48 h on 24 compute nodes (1152 cores). The high computational cost of performing a quantum mechanical calculation is balanced by the wealth of information that can be accessed, including structural, mechanical, magnetic, and optical properties. For example, heats of formation can be used to screen hypothetical compositions,¹³ the strength of electron–exchange interactions can be used to predict magnetic critical temperatures,¹⁴ and the composition of frontier orbitals can be used to explain catalytic activity.¹⁵

Electronic structure: More than a sum of parts

A wide variety of MOFs have been reported with organic and inorganic networks ranging from zero to three dimensions of connectivity.¹⁶ For example, the hybrid halide perovskites that are being intensively studied for applications in solar-energy conversion can be considered as the combination of a three-dimensional (3D) anionic inorganic framework with a zero-dimensional (0D) cationic molecular sublattice.¹⁷ For conciseness, we restrict our present discussion to standard porous MOFs with 3D inorganic–organic–inorganic connectivity (as found in the ubiquitous MOF-5 that combines a cationic zinc oxide subunit connected by anionic benzene dicarboxylate linkers to form a 3D porous framework [see **Figure 1a**, center]).

The orbital composition and spatial location of the valence and conduction bands determines most equilibrium properties of materials. The electronic structure of most MOFs can be described in a manner similar to molecular orbital diagrams common to organometallic chemistry. However, the diverse chemistry of both the organic linkers and the inorganic nodes—for example, whether the node includes

an inorganic cation like the Zn_4O^{6+} cluster of the isorecticular (IRMOF) series—can require more detailed considerations. In particular, interesting chemistry occurs at the inorganic–organic interface. While studied in detail in the context of surface science and molecular catalysis, the concepts of matching electronic energy levels and orbital symmetry are rarely invoked in MOF chemistry.

An electronic structure calculation can provide insights into the composition, energy, and distribution of the frontier extended orbitals (electronic band edges) of any compound. Consider three of the most widely studied MOFs: Zr–UiO-66 (University of Oslo),¹⁸ Zn–MOF-5,¹⁹ and Ti–MIL-125 (Materials Institut Lavoisier).²⁰ Each framework features a closed-shell s^0 or d^0 metal connected by benzene dicarboxylate linkers. The band edges, however, are the product of the chemistry involving the ligand, metal, and their interface as shown in **Figure 1**. In the case of Zr–UiO-66 and Zn–MOF-5, both the valence and conduction bands are defined by organic orbitals. Thus, organic functionalization can be used to modify the chemistry of the band edges^{15,21} and the physical properties of the

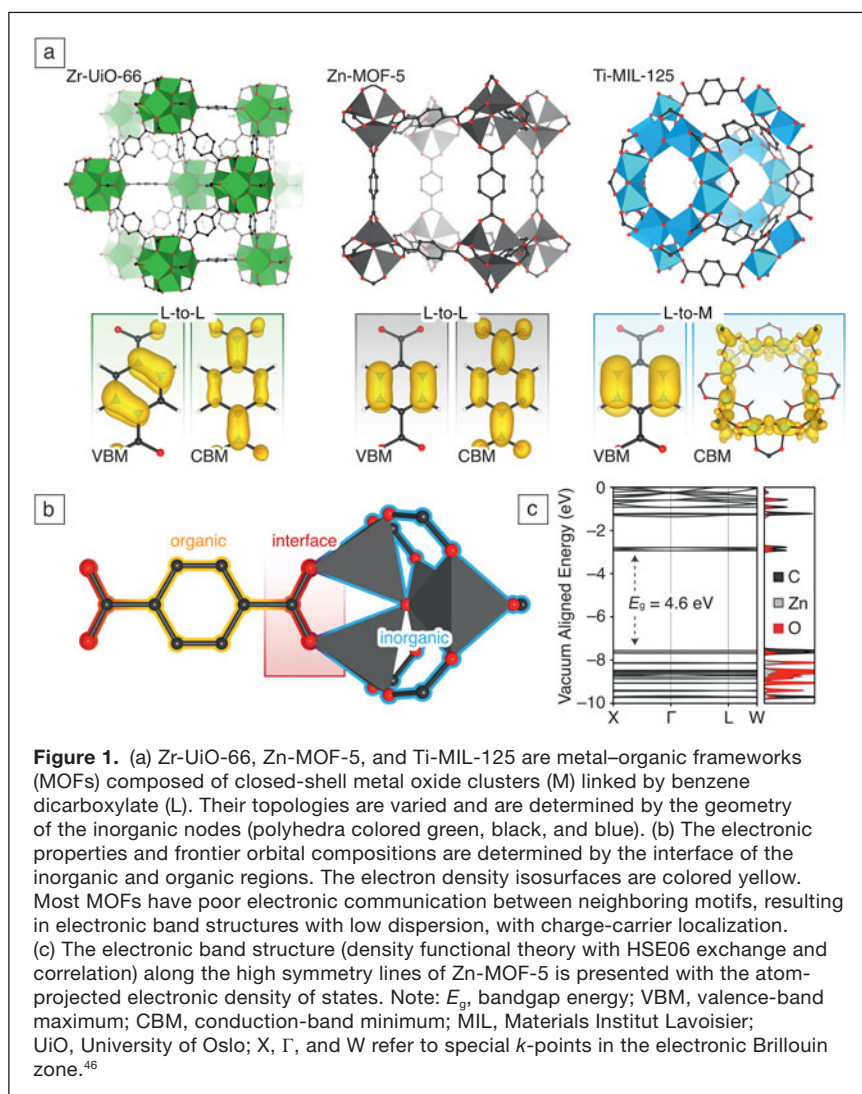


Figure 1. (a) Zr–UiO-66, Zn–MOF-5, and Ti–MIL-125 are metal–organic frameworks (MOFs) composed of closed-shell metal oxide clusters (M) linked by benzene dicarboxylate (L). Their topologies are varied and are determined by the geometry of the inorganic nodes (polyhedra colored green, black, and blue). (b) The electronic properties and frontier orbital compositions are determined by the interface of the inorganic and organic regions. The electron density isosurfaces are colored yellow. Most MOFs have poor electronic communication between neighboring motifs, resulting in electronic band structures with low dispersion, with charge-carrier localization. (c) The electronic band structure (density functional theory with HSE06 exchange and correlation) along the high symmetry lines of Zn–MOF-5 is presented with the atom-projected electronic density of states. Note: E_g , bandgap energy; VBM, valence-band maximum; CBM, conduction-band minimum; MIL, Materials Institut Lavoisier; UiO, University of Oslo; X, Γ , and W refer to special k -points in the electronic Brillouin zone.⁴⁶

material.²² Alternatively, the chemically inert ZrO₂-based node found in UiO-66 and compositionally similar analogues, such as NU-1000²³ (Northwestern University), can be used to anchor catalytically active metals, providing access to heterogeneous catalysts.²⁴ Similar metal anchoring is possible through ligand substitutions that enhance coordinating functionality (e.g., amines, thiols, and alcohols).²⁵

Owing to its wide optical bandgap in the UV range ($E_g \sim 4.6$ eV) and high binding energy Zn₄O⁶⁺-derived bands (-8.1 eV below vacuum level—significantly deeper than the valence-band edge), Zn-MOF-5 offers a further level of chemical modularity allowing for band tuning through both organic functionalization, as well as through metal exchange at the Zn sites. Substitutions for other d-block metals can install mid-gap metal-centered states that result in the MOF featuring a metal-to-ligand transition.²⁶ Such cationic substitutions have been proposed in the UiO-type materials, although it remains an open question whether the metals exchange or are anchored to the node.

Ti-MIL-125 provides interesting avenues for chemical functionalization because the excitation from the ligand to metal cluster creates a transient Ti(III) center, which is stable for up to 900 ps.¹⁵ Moreover, unmodified Ti-MIL-125 features a bandgap ($E_g \sim 3.8$ eV) that is tunable with simple organic functionalization.²⁷

The chemical modularity of these frameworks reflects their metastability and the chemical softness of the ligand–metal interface. The downside is that many frameworks decompose in the presence of nucleophiles. Furthermore, weak electronic interaction at their interface results in flat electronic bands (large effective masses for electrons and holes) that are localized in real space.

From electron energies to band diagrams

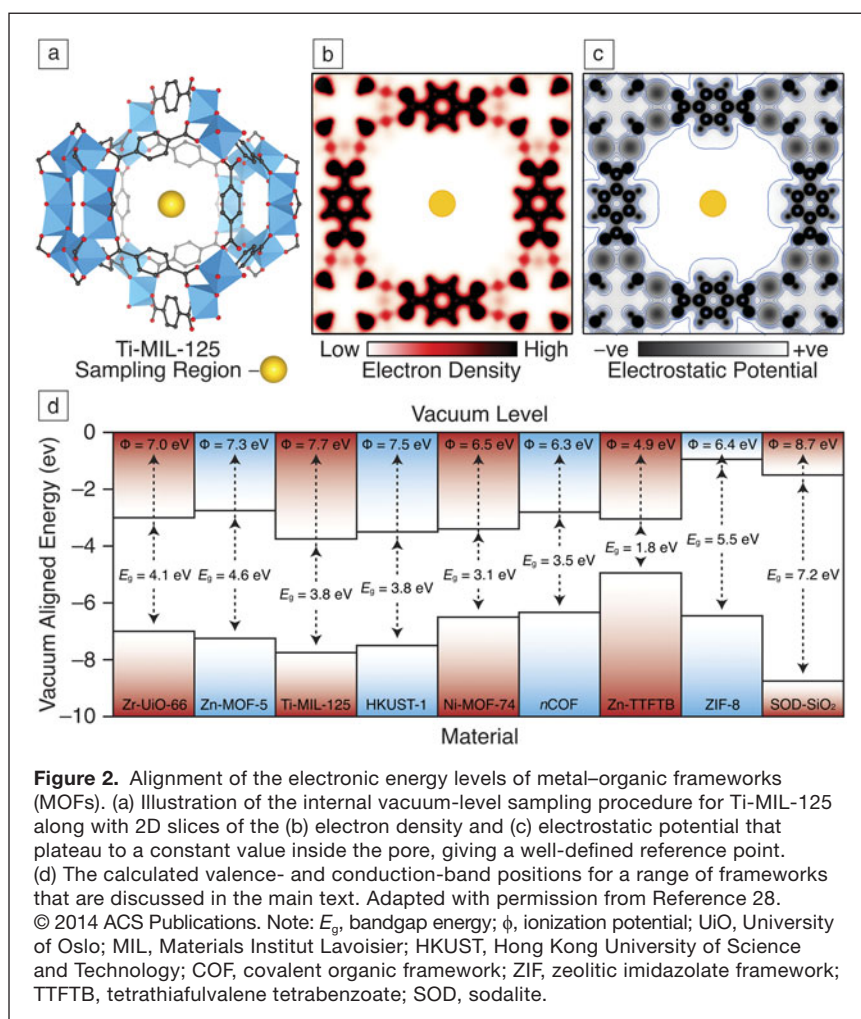
Knowing the electronic structure of a material can provide useful guidelines for design. The next step, in order to be able to consider a material in a device context, is to place the electron energies on an absolute scale, thus facilitating the construction of energy-band diagrams (Figure 2).²⁸ The construction of band diagrams is a cornerstone of semiconductor device design, as one of the pioneers of heterojunction design H. Kroemer famously stated that “If, in discussing a semiconductor problem, you cannot draw an energy-band diagram, this shows that you don’t know what you are talking about.”²⁹

While ionization potential (electron removal energy) and electron affinity (electron addition energy) are properties that are easily defined for solids, they are difficult to quantify. It was recognized as early as the 1930s that the photoelectric threshold of solids is influenced

by two factors: the bulk band energies and the surface electrostatic double layer.³⁰ Due to the sensitivity of the surface term to the processing history, environment, and morphology of a particular sample, there is a large variation in reported values for a given compound.

Similarly, for theorists, the use of periodic boundary conditions introduces problems in predicting reliable electron energies. While periodic boundaries offer a convenient and elegant route to representing an infinite crystal from a finite repeating unit, the solution of the Coulomb interactions introduces an arbitrary reference point for the electrostatic potential, meaning that band energies cannot be compared directly between systems.^{31–33} In another approach, the crystal can be modeled by considering a representative cluster of finite size, which provides an external vacuum level and facilitates comparison of band energies between systems;^{34,35} however, in practice, the models are challenging to construct for multicomponent systems.

In this context, we formulated a new procedure to calculate the bulk band energies of porous solids.²⁸ The method is based on a periodic DFT approach and samples the electrostatic potential at the center of a pore where the electron density has decayed to zero and the electrostatic potential has a plateau



(see Figure 2). The procedure, which is applicable to porous solids, is analogous to the use of the external vacuum level above a surface slab as a reference in solid-state calculations. The center of large pores is also a vacuum that provides a reference level for alignment between different materials.

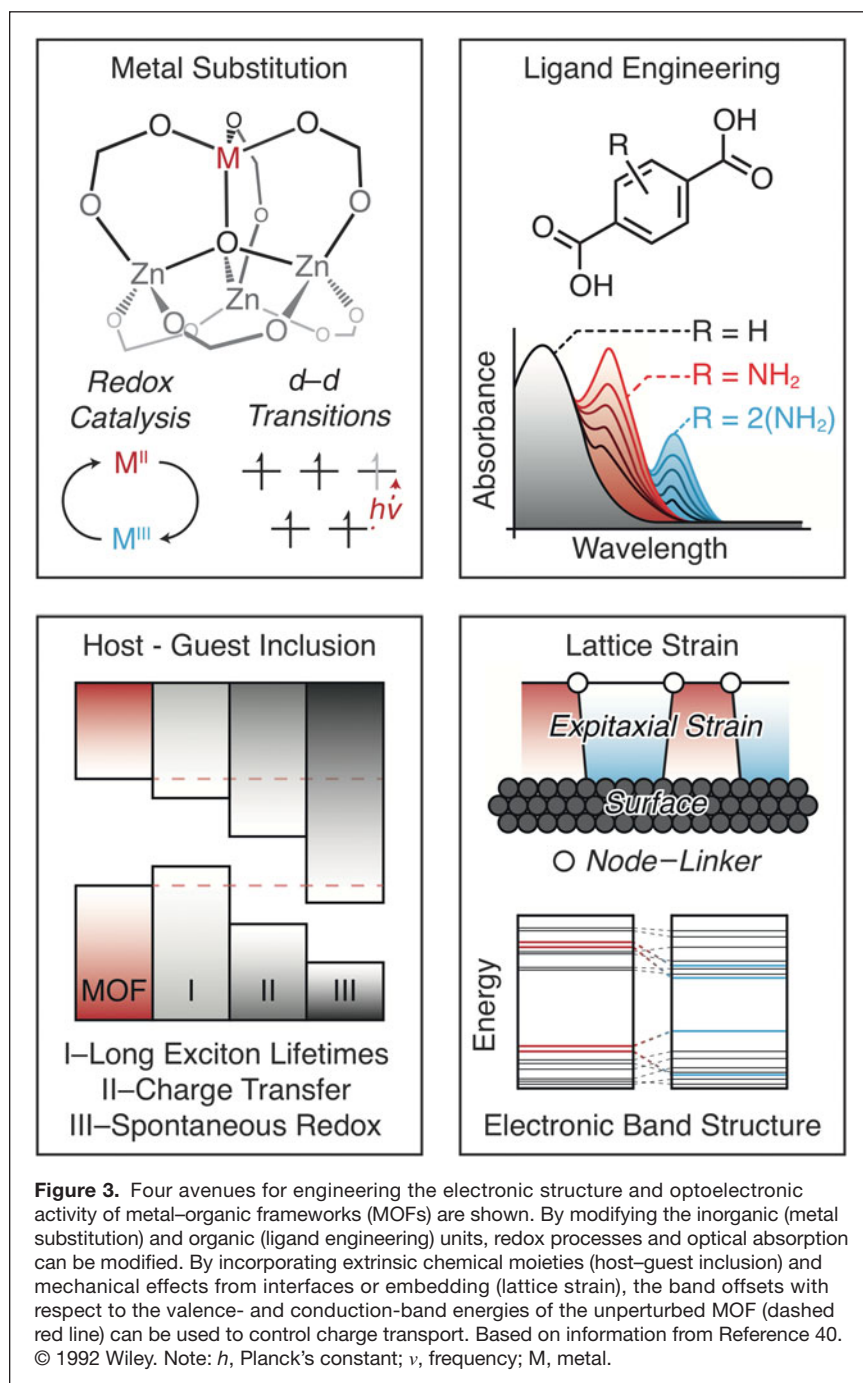
Practically, the alignment is achieved by performing a periodic electronic structure calculation at a given level of theory. The level of theory will affect the reliability of the results, and a hybrid exchange-correlational functional (or beyond) is recommended for quantitative insights. The electrostatic (Hartree) potential at the center of the largest pore is then evaluated; this can be achieved using the MacroDensity³⁶ package, which we have developed for this purpose. One must ensure that the integrated value of the potential has reached a reliable convergence, which is achieved by sampling a large enough area (a sphere of radius $> 2 \text{ \AA}$) and ensuring that the variance within the sampling volume is small ($< 0.01 \text{ V}$). The Hartree potential obtained is now referred to as the vacuum potential (V_{vac}). The ionization potential is simply determined by subtracting the highest occupied band eigenvalue (E_{VB}): $IP = V_{\text{vac}} - E_{\text{VB}}$. Similarly, the electron affinity is determined using the lowest unoccupied band eigenvalue (E_{CB}). The resultant ionization potentials and electron affinities can be compared across all materials.

Access to absolute band energies allows for the design of a range of physical applications for MOFs. Recently, Cheng et al. found that using a newly designed ligand, they could obtain a material, which electronic structure calculations predict to have band energies suitable for hydrolysis and degradation of organic pollutants.³⁷ Moreover, they experimentally demonstrated the strong photocatalytic activity of the resulting material. The alignment of energy levels has also been applied to explain the differences in photocatalytic activity in d^0 MOFs.¹⁵ Graucrespo and co-workers demonstrated control of frontier orbital positions by metal substitution in porphyrin-containing MOFs, allowing crystal engineering for solar-fuel production.³⁸ In the context of device design, access to absolute energy levels, as well as lattice parameters from sources such as the CoRE-MOF database, will allow for the application of design strategies such as the recently developed electronic-lattice-site (ELS) metric³⁹—which measures the quality of heterostructure interfaces—to fulfill the conditions of Kroemer's lemma. These developments open the field for the design of heterojunctions featuring MOFs.

Principles for electroactivation

We now collate design principles for tailoring the physical properties. The critical criterion for realizing semiconducting MOFs is that the frontier electronic bands are delocalized (low-carrier effective masses), which requires effective communication between the organic and inorganic building blocks. However, long-range transport is not always essential, and short-range electron transfer (e.g., to an electrolyte at the surface or penetrating the pore) can be sufficient to support a wide range of redox processes.

A set of four chemical principles for electroactivation of MOFs is outlined in Figure 3.⁴⁰ These range from modifying



the organic and inorganic building blocks that form the framework to post-synthetic modification and the application of lattice and chemical strain.

Metal substitution

Depending on the chemical identity and charge state, the orbitals of the metal may form the upper valence or lower conduction band of the MOF. Therefore, metal substitution has the potential to influence both oxidation (hole injection) and reduction (electron injection) processes. For example, in HKUST-1 (Hong Kong University of Science and Technology), the Cu 3*d* orbitals are found at the valence-band maximum,⁴¹ while in MIL-125, the Ti 3*d* orbitals are found at the conduction-band minimum. Beyond complete metal substitution, the formation of mixed-metal systems offers a promising route to tune redox activity. Brozek and Dincă demonstrated this for MOF-5 with Ti, V, Cr, Mn, and Fe incorporation.²⁶

Ligand engineering

The choice of ligand can be used to tune the electronic structure directly by modifying the orbital composition or indirectly by changing the framework topology. Many MOFs have at least one frontier band centered on an organic conjugated region. The electron energies of the organic regions are therefore tunable using conventional “push-pull” principles, where the band energies are influenced by the electron-donating or withdrawing capability of additional substituents. For example, the introduction of an electron-donating primary amine to a benzene ring will result in an enhancement of electron density and a lowering of the ionization potential. Amination has been effective at introducing visible light photoactivity in a range of simple MOFs by raising the valence-band energy (e.g., modification of benzene dicarboxylate in MIL-125²⁷ and UiO-66).¹⁵ As an alternative to ligand modification, different types of ligands are being explored (e.g., linear conjugated carboxylates have been shown to exhibit extended helical orbitals⁴² with the potential for long-range magnetic coupling).⁴³

Host-guest inclusion

The introduction of redox active molecular guests into a framework is one method to change the electronic properties, either through spontaneous or through light-activated charge transfer. A related process is the ability to “rewire” an insulating MOF through an auxiliary electroactive linker. The champion system in this regard is HKUST-1 modified with the molecule TCNQ (7,7,8,8-tetracyanoquinodimethane) that provided a route to tunable conductivity.⁴⁴ Allen and Cohen recently demonstrated cross-linking in a series of isoreticular MOFs,²² which could be extended to install conductive pathways for a wider range of MOF topologies.

Lattice strain

A feature of porous frameworks is that they are mechanically soft and flexible in comparison to close-packed materials, which provides another route to engineer their properties. Stress and strain can be introduced in MOFs in several ways, such as by epitaxial growth on a rigid substrate, solid-state embedding of MOF particles in a host, and the application of pressure, either mechanically or chemically (e.g., defects such as missing ligands are sensitive to the growth conditions and reagents).⁴⁵ The electronic structure response is described by the deformation potential: the change in ionization potential, electronic affinity, or bandgap with respect to a volume (pressure) change. It has been shown that the volume deformation potential is comparable to inorganic semiconductors;⁴⁶ however, critically, due to smaller bulk moduli, the effects of pressure on the band gap is much larger. In the compound nCOF-1 (nCOF, noncovalent framework), the bandgap change of -2.2 eV/GPa is 20× larger than for bulk Si.⁴⁷ For these materials, a small external stimulus can result in a large change in the electronic structure.

Summary and outlook

Our discussion has focused on the successes of modern simulation techniques in describing the chemical bonding and physical properties of MOFs. While recent progress has been substantial, the *a priori* design of functional hybrid solids remains a daunting challenge. We have outlined fertile avenues for the pursuit of materials where the injection, extraction, excitation, and transport of charge carriers are controllable, which build on the hybrid compounds reported in the articles in this issue. Not only can the composition of the framework itself be engineered, the porosity can also be exploited for adsorbate interactions that activate optical or electronic activity.

The approaches we have outlined for engineering physical properties can be exploited for the use of MOFs in a range of devices where the hybrid advantage offers the prospect of disruptive technologies. With the number of peer-reviewed papers on conductive MOFs rapidly increasing, a roadmap for future progress is illustrated in **Figure 4**,⁴⁸ drawing from an

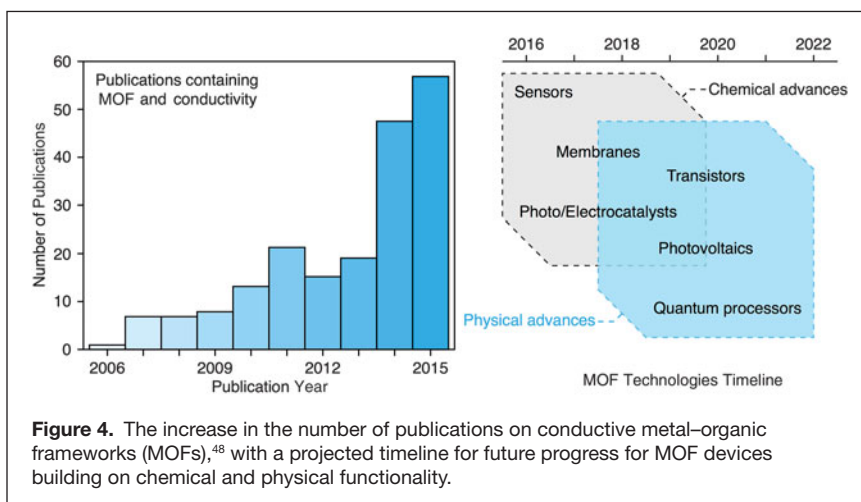


Table I. Potential applications for electroactive metal–organic frameworks, with key physical properties and potential for input from materials modeling.

Application	Physical Property	Modeling Input
Photocatalyst	Redox potentials	Band-edge positions
	Optical absorption	Optical bandgaps
	Reactivity	Reaction barriers
Sensor	Analyte selectivity	Absorption isotherms
	Signal processing	Elastic tensors
	Conductivity change	Deformation potentials
Membrane	Ion transport	Diffusion constants
	Selectivity	Absorption isotherms
	Film quality	Substrate epitaxy
Solar cells	Optical absorption	Optical bandgaps
	Carrier transport	Effective mass
	Carrier concentrations	Defect concentrations
	Contact resistance	Band-edge positions
Transistors	Carrier mobility	Effective mass
	Film quality	Substrate epitaxy
	Contact resistance	Band offsets

earlier perspective of Allendorf et al.⁴⁹ In **Table I** we list several possibilities that highlight the potential role for materials modeling. Referring back to the Nobel lecture of H. Kroemer: “The principal applications of any sufficiently new and innovative technology have always been—and will continue to be—applications created by that technology.”

Acknowledgments

We thank W. Kohn and H. Kroto for the development of density functional theory and physical properties of MOF chemistry, respectively, as well as for stimulating lectures and discussions on these topics. The research discussed here has benefited from collaboration with J.K. Bristow, D. Tiana, and K.L. Svane. We acknowledge support from The Royal Society, the European Research Council (Grant No. 27757) and the EPSRC (Grant No. EP/M009580/1 and EP/K016288/1). This work used the Extreme Science and Engineering Discovery Environment (XSEDE), which is supported by the National Science Foundation Grant Number ACI-1053575.

References

1. K. Lejaeghere, T. Björkman, P. Blaha, S. Blügel, V. Blum, D. Caliste, I.E. Castelli, S.J. Clark, A. Dal Corso, S. de Gironcoli, T. Deutsch, J.K. Dewhurst, I. Di Marco, C. Draxl, M. Duktak, O. Eriksson, J.A. Flores-Livas, K.F. Garrity, L. Genovese, P. Giannozzi, M. Giantomassi, S. Goedecker, X. Gonze, O. Grånäs, E.K.U. Gross, A. Gulans, F. Gygi, D.R. Hamann, P.J. Hasnip, N.A.W. Holzwarth, D. Iuşan, D.B. Jochym, F. Jollet, D. Jones, G. Kresse, K. Koepnick, E. Küçükbenli, Y.O. Kvashnin, I.L.M. Locht, S. Lubeck, M. Marsman, N. Marzari, U. Nitzsche, L. Nordström, T. Ozaki, L. Paulatto, C.J. Pickard, W. Poelmans, M.I.J. Probert, K. Refson, M. Richter, G.-M. Rignanese, S. Saha, M. Scheffler, M. Schlipf, K. Schwarz, S. Sharma, F. Tavazza, P. Thunström, A. Tkatchenko, M. Torrent, D. Vanderbilt, M.J. van Setten, V. Van Speybroeck, J.M. Wills, J.R. Yates, G.-X. Zhang, S. Cottenier, *Science* **351**, 1 (2016).

2. K.T. Butler, J.M. Frost, J.M. Skelton, K.L. Svane, A. Walsh, *Chem. Soc. Rev.*, published online March 18, 2016, <http://dx.doi.org/10.1039/C5CS00841G>.
3. C.E. Wilmer, M. Leaf, C.Y. Lee, O.K. Farha, B.G. Hauser, J.T. Hupp, R.Q. Snurr, *Nat. Chem.* **4**, 83 (2011).
4. <http://gregchung.github.io/CoRE-MOFs>.
5. Y.G. Chung, J. Camp, M. Haranczyk, B.J. Sikora, W. Bury, V. Krungleviciute, T. Yildirim, O.K. Farha, D.S. Sholl, R.Q. Snurr, *Chem. Mater.* **26**, 6185 (2014).
6. M.T. Dove, *Am. Mineral.* **82**, 213 (1997).
7. G. Kieslich, A.C. Forse, S. Sun, K.T. Butler, S. Kumagai, Y. Wu, M.R. Warren, A. Walsh, C.P. Grey, A.K. Cheetham, *Chem. Mater.* **28**, 312 (2016).
8. G. Kieslich, S. Kumagai, K.T. Butler, T. Okamura, C.H. Hendon, S. Sun, M. Yamashita, A. Walsh, A.K. Cheetham, *Chem. Commun.* **51**, 15538 (2015).
9. A.M.A. Leguy, J.M. Frost, A.P. McMahon, V. Garcia Sakai, W. Kockelmann, C.H. Law, X. Li, F. Foglia, A. Walsh, B.C. O'Regan, J. Nelson, J.T. Cabral, P.R.F. Barnes, *Nat. Commun.* **6**, 7124 (2015).
10. F. Brivio, J.M. Frost, J.M. Skelton, A.J. Jackson, O.J. Weber, M.T. Weller, A.R. Goñi, A.M.A. Leguy, P.R.F. Barnes, A. Walsh, *Phys. Rev. B Condens. Matter* **92**, 144308 (2015).
11. A.B. Cairns, A.L. Goodwin, *Chem. Soc. Rev.* **42**, 4881 (2013).
12. J.P. Perdew, A. Ruzsinszky, G.I. Csonka, O.A. Vydrov, G.E. Scuseria, L.A. Constantin, X. Zhou, K. Burke, *Phys. Rev. Lett.* **100**, 136406 (2008).
13. C.H. Hendon, D. Tiana, T.P. Vaid, A. Walsh, *J. Mater. Chem. C* **3**, 95 (2013).
14. K. Svane, P.J. Saines, A. Walsh, *J. Mater. Chem. C* **3**, 11076 (2015).
15. M. Nasalevich, C.H. Hendon, J.G. Santaclara, K. Svane, B. van der Linden, S.L. Veber, M.V. Fedin, A.J. Houtepen, M.A. van der Veen, F. Kaptejin, A. Walsh, J. Gascon, *Sci. Rep.* **6**, 23676 (2016).
16. A.K. Cheetham, C.N.R. Rao, R.K. Feller, *Chem. Commun.* **46**, 4780 (2006).
17. J.M. Frost, K.T. Butler, F. Brivio, C.H. Hendon, M. van Schilfgarde, A. Walsh, *Nano Lett.* **14**, 2584 (2014).
18. J.H. Cavka, S. Jakobsen, U. Olsbye, N. Guillou, C. Lamberti, S. Bordiga, K.P. Lillerud, *J. Am. Chem. Soc.* **130**, 13850 (2008).
19. H. Li, M. Eddaoudi, M. O'Keeffe, O.M. Yaghi, *Nature* **402**, 276 (1999).
20. M. Dan-Hardi, C. Serre, T. Frot, L. Rozes, G. Maurin, C. Sanchez, G. Férey, *J. Am. Chem. Soc.* **131**, 10857 (2009).
21. L. Shen, R. Liang, M. Luo, F. Jing, L. Wu, *Phys. Chem. Chem. Phys.* **17**, 117 (2015).
22. C.A. Allen, S.M. Cohen, *Inorg. Chem.* **53**, 7014 (2014).
23. J.E. Mondloch, W. Bury, D. Fairen-Jimenez, S. Kwon, E.J. DeMarco, M.H. Weston, A.A. Sarjeant, S.T. Nguyen, P.C. Stair, R.Q. Snurr, O.K. Farha, J.T. Hupp, *J. Am. Chem. Soc.* **135**, 10294 (2013).
24. D. Yang, S.O. Odoh, T.C. Wang, O.K. Farha, J.T. Hupp, C.J. Cramer, L. Gagliardi, B.C. Gates, *J. Am. Chem. Soc.* **137**, 7391 (2015).
25. H. Fei, S.M. Cohen, *J. Am. Chem. Soc.* **137**, 2191 (2015).
26. C.K. Brozek, M. Dincă, *J. Am. Chem. Soc.* **135**, 12886 (2013).
27. C.H. Hendon, D. Tiana, M. Fontecave, C. Sanchez, L. D'arras, C. Sassoie, L. Rozes, C. Mellot-Draznieks, A. Walsh, *J. Am. Chem. Soc.* **135**, 10942 (2013).
28. K.T. Butler, C.H. Hendon, A. Walsh, *J. Am. Chem. Soc.* **136**, 2703 (2014).
29. H. Kroemer, Nobel Lecture, “Quasi-Electric Fields and Band Offsets: Teaching Electrons New Tricks” (2000).
30. J. Bardeen, *Phys. Rev.* **49**, 635 (1936).
31. A. Walsh, K.T. Butler, *Acc. Chem. Res.* **47**, 364 (2014).
32. E. Smith, *Physica A* **120A**, 327 (1983).
33. J. Ihm, A. Zunger, M. Cohen, *J. Phys. C Solid State Phys.* **12**, 4409 (1979).
34. J. Buckeridge, K.T. Butler, C.R.A. Catlow, A.J. Logsdail, D.O. Scanlon, S.A. Shevlin, S.M. Woodley, A.A. Sokol, A. Walsh, *Chem. Mater.* **27**, 3844 (2015).
35. D.O. Scanlon, C.W. Dunnill, J. Buckeridge, S.A. Shevlin, A.J. Logsdail, S.M. Woodley, C.R.A. Catlow, M.J. Powell, R.G. Palgrave, I.P. Parkin, G.W. Watson, T.W. Keal, P. Sherwood, A. Walsh, A.A. Sokol, *Nat. Mater.* **12**, 798 (2013).
36. <https://github.com/WMD-group/MacroDensity>.
37. Z.-L. Wu, C.-H. Wang, B. Zhao, J. Dong, F. Lu, W.-H. Wang, W.-C. Wang, G.-J. Wu, J.-Z. Cui, P. Cheng, *Angew. Chem. Int. Ed. Engl.* **55**, 4938 (2016).
38. S. Hamad, N.C. Hernandez, A. Aziz, A.R. Ruiz-Salvador, S. Calero, R. Grau-Crespo, *J. Mater. Chem. A* **3**, 23458 (2015).
39. K.T. Butler, Y. Kumagai, F. Oba, A. Walsh, *J. Mater. Chem. C* **4**, 1149 (2016).
40. G.A. Ozin, *Adv. Mater.* **4**, 612 (1992).
41. C.H. Hendon, A. Walsh, *Chem. Sci.* **6**, 3674 (2015).

42. C.H. Hendon, D. Tiana, A.T. Murray, D.R. Carbery, A. Walsh, *Chem. Sci.* **4**, 4278 (2013).
 43. D. Tiana, C. Hendon, A. Walsh, *Chem. Commun.* **50**, 13990 (2014).
 44. A.A. Talin, A. Centrone, A.C. Ford, M.E. Foster, V. Stavila, P. Haney, R.A. Kinney, V. Szalai, F. El Gabaly, H.P. Yoon, F. Léonard, M.D. Allendorf, *Science* **343**, 6166 (2014).
 45. J.K. Bristow, K.L. Svane, D. Tiana, J.M. Skelton, J.D. Gale, A. Walsh, *J. Phys. Chem. C* **120**, 9276 (2016).
 46. K.T. Butler, C.H. Hendon, A. Walsh, *ACS Appl. Mater. Interfaces* **6**, 22044 (2014).
 47. C.H. Hendon, K.E. Wittering, T.-H. Chen, W. Kaveevitvichai, I. Popov, K.T. Butler, C.C. Wilson, D.L. Cruickshank, O.Š. Miljanić, A. Walsh, *Nano Lett.* **15**, 2149 (2015).
 48. Web of Science, June 2016.
 49. M.D. Allendorf, A. Schwartzberg, V. Stavila, A.A. Talin, *Chem. Eur. J.* **17**, 11372 (2011). □



Keith T. Butler is in the Department of Chemistry at the University of Bath. He received his BA degree in medicinal chemistry from Trinity College, Dublin and PhD degree in computational chemistry from University College London. Following postdoctoral research at the University of Sheffield on silicon solar cells, Butler joined the UK SUPERSOLAR Project at Bath to focus on next-generation materials for solar-energy conversion. Butler can be reached by phone at +44 1225384913 or by email at k.t.butler@bath.ac.uk.



Aron Walsh is a professor of materials design at Imperial College London. He received his BA and PhD degrees in chemistry from Trinity College, Dublin, and held positions at the National Renewable Energy Laboratory, University College London, and the University of Bath. In 2015, he was awarded the EU-40 Materials Prize from the European Materials Research Society for his work on perovskite solar cells. His research focuses on the theory and simulation of functional materials. Walsh can be reached by email at a.walsh@imperial.ac.uk.



Christopher H. Hendon is a postdoctoral researcher at the Massachusetts Institute of Technology. He received his BSc degree in chemistry from Monash University, Australia, and his PhD degree from the University of Bath. His research interests include the physical chemistry of metal–organic frameworks. Hendon can be reached by phone at 617-324-2161 or by email at hendon@mit.edu.

give to the causes you care about

www.mrs.org/foundation

Leading With Innovation

TALC? I DON'T THINK SO! WHOLE PATTERN FITTING

Many products are not regulated by a governing body. Quality control is in the hands of those who use these products. For example, Figure 1 shows a white powder from a bottle labeled "talc." When this powder was run on the MiniFlex, talc was observed only in trace quantities (Figure 2). Talc is typically identified as magnesium silicate hydroxide. However, this material is primarily composed of calcite and dolomite identified as calcium/magnesium carbonate (Figure 3).

Figure 1: Talc

Figure 2: X-ray Diffractogram of Talc | Cu ka radiation (30 kV, 15 mA)
 Counting statistics: 0.02 deg/step with a 3 sec. dwell time

This material was intended to be used as a drying agent; therefore the intended use is still possible. However, if you were looking for a silicate source, you would not find it here.

Figure 3: Whole Pattern Fitting Analysis

APP BYTE
 Rigaku Corporation and its Global Subsidiaries
 www.Rigaku.com | info@Rigaku.com

MRS Booth 712